ChemPubSoc Europe

DOI: 10.1002/chem.201406170

CHEMISTRY A European Journal Full Paper

Vesicles |*Hot Paper*|

Unilamellar Vesicles from Amphiphilic Graphene Quantum Dots

Sukhendu Nandi,[b] Sofiya Kolusheva,[a] Ravit Malishev,[b] Alexander Trachtenberg,[b] T. P. Vinod,[b] and Raz Jelinek*[a, b]

Abstract: Graphene quantum dots (GQDs) have attracted considerable interest due to their unique physicochemical properties and various applications. For the first time it is shown that GQDs surface-functionalized with hydrocarbon chains (i.e., amphiphilic GQDs) self-assemble into unilamellar spherical vesicles in aqueous solution. The amphiphilic GQD vesicles exhibit multicolor luminescence that can be readily exploited for membrane studies by fluorescence spectroscopy and microscopy. The GQD vesicles were used for microscopic analysis of membrane interactions and disruption by the peptide beta-amyloid.

Introduction

Graphene quantum dots (GQDs) are carbon nanoparticles consisting of crystalline graphitic cores. These carbonaceous nanoparticles have attracted significant interest due to their unique structural and photophysical properties, as well as applications in nanobiotechnology.[1] GQDs exhibit a broad color range (e.g., excitation/emission wavelength pairs),[2] fluorescence upconversion,[3] and high quantum yield.[1b,4] The graphitic cores of GQDs can be chemically functionalized, and GQDs displaying various molecular units have been reported.[5] In particular, GQDs derivatized with extended hydrocarbon chains, that is, amphiphilic GQDs, exhibit pronounced photophysical sensitivity to the nature of organic solvents[4,6] and have been used as fluorescent membrane markers[7] and for creating multicolor printing patterns.[5b,8]

Almost all GQD systems reported thus far have involved individual GQDs in solution, but there have been no reports on self-assembled structures composed of GQDs. Here we demonstrate for the first time that amphiphilic GQDs form spherical unilamellar vesicles in aqueous solution. The amphiphilic GQD vesicles resemble conventional unilamellar lipid assemblies in their overall morphology; however, an important advantage arises from the luminescence properties of the GQDs, which make the vesicular assemblies a powerful platform for analysis of membrane processes. As a representative example, we describe application of the GQD vesicles for microscopic analysis of membrane transformations induced by beta-amyloid, a prominent membrane-active peptide closely associated with the pathology of Alzheimer's disease.[9]

[a] *S. Kolusheva, R. Jelinek*
Ilse Katz Institute for Nanoscale Science & Technology
Ben Gurion University of the Negev
Beer Sheva 84105 (Israel)

[b] *S. Nandi, R. Malishev, A. Trachtenberg, T. P. Vinod, R. Jelinek*
Department of Chemistry
Ben Gurion University of the Negev
Beer Sheva 84105 (Israel)
Fax: (+972) 8-6472943
E-mail: razj@bgu.ac.il

Supporting information for this article is available on the WWW under http://dx.doi.org/10.1002/chem.201406170.

Results and Discussion

Amphiphilic GQDs were synthesized through modification of previously reported schemes (Figure 1 of the Supporting Information). Briefly, oxidative cleavage of carbon fibers in an acidic environment generated GQDs having carboxyl residues, which underwent acid-catalyzed esterification in the presence of stearyl alcohol as nucleophile to give amphiphilic GQDs[5b,10] (Figure 1 SI in the Supporting Information). NMR (Figure 2 SI in the Supporting Information) and FTIR spectroscopy (Figure 3 SI in the Supporting Information) confirmed attachment of 1-octadecanol side chains to the GQDs.

The TEM images presented in Figure 1 show a fairly uniform size distribution of the amphiphilic GQDs and confirm the crystallinity of their graphitic cores. Specifically, high-resolution TEM (HRTEM) analysis (Figure 1 A, B) indicated that the average diameter of the amphiphilic GQDs was (2.4 ± 0.1) nm. HRTEM examination of a single dot (Figure 1 B) underscored the crystalline core with a lattice parameter of 0.242 nm, which corresponds to the 1120 facet of graphene.[1a] AFM (Figure 1 D, E) revealed a particle height of (0.7 ± 0.1) nm, that is, the GQD cores consist of two graphene layers,[11] as has been previously observed in many GQD systems.

The amphiphilic GQDs spontaneously assembled into spherical vesicles through a simple procedure in which the nanoparticles were dissolved in an organic solvent, dried, re-solubilized in water, and subjected to rapid evaporation (see Experimental Section).[12] The vesicles could be easily discerned by light microscopy and were stable for long periods (4–6 h). Amphiphilic molecules such as phospholipids and sterols readily form vesicles in aqueous solution, and such self-assembled biomimetic bilayer structures are fundamental vehicles for studying biolog-

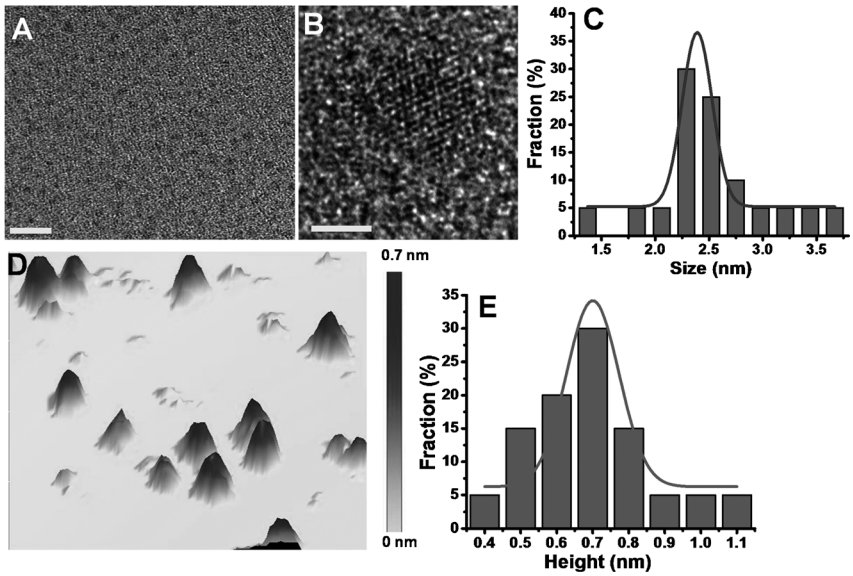

Figure 1. Microscopic analysis of amphiphilic GQDs. A) HRTEM image of amphiphilic GQDs. Scale bar: 10 nm; B) HRTEM image of a single amphiphilic GQD showing the crystal planes. Scale bar: 2 nm. C) Size distribution of the amphiphilic GQDs shown in A) obtained by application of image analysis algorithms. D) AFM image of amphiphilic GQDs on mica. E) Statistical analysis of the particle heights recorded in the AFM experiment.

ical membranes and membrane processes.[13] Inorganic nanoparticles coated with surfactant molecules have also been shown to form micellar structures and vesicles in water.[14] The amphiphilic GQD vesicles formed in water are, to the best of our knowledge, the first example of vesicular assemblies obtained from carbon nanoparticles.

Figure 2 shows experimental characterization of the new GQD vesicles. We emphasize that the vesicles depicted in Figure 2 consist of only GQDs, with no added surfactant or lipid stabilizers. Cryogenic TEM (cryo-TEM, Figure 2A) and cryo-SEM (Figure 2B) show the spherical, unilamellar organization of the vesicles. Specifically, both cryo-TEM images of the population of smaller vesicles obtained after centrifugation and cryo-SEM images showing larger vesicles in Figure 2A and B clearly show that the vesicles are bordered by a single GQD layer. The small-angle X-ray scattering (SAXS) spectrum in Figure 2C indicates a lamellar thickness of approximately 5.4 nm (Figure 2C). This value is consistent with a bilayer organization of two stacked GQDs having partly overlapping hydrocarbon side chains. The overall size of a single amphiphilic GQD comprising a graphite core of about 0.7 nm in height (Figure 1C) and extended 1-octadecanol chains, the length of which is around 2.3 nm, is approximately 3 nm.[15]

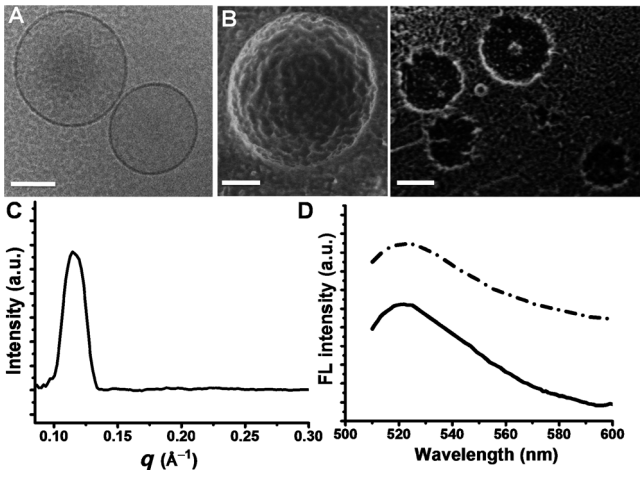

Figure 2. Characterization of amphiphilic GQD vesicles. A) Cryo-TEM image. Scale bar: 100 nm. B) Cryo-SEM image. Scale bars correspond to 0.5 (left) and 1 μm (right). C) SAXS spectrum. D) Fluorescence leakage experiment depicting fluorescence emission (excitation at 495 nm) of amphiphilic GQD vesicles embedding fluorescein before (solid curve) and after (dash-dotted curve) addition of 10 μL of 10% (w/v) Triton X-100 to the vesicles.

A fluorescence leakage experiment[16] (Figure 2D) further attested to the unilamellar vesicle architecture, in which an aqueous solution is confined within the GQD lamellae. Specifically, the initial fluorescence emission of fluorescein encapsulated within the amphiphilic GQD vesicles is lower due to self-quenching occurring in the enclosed volume. However, significantly increased fluorescence was recorded after addition of a detergent (Figure 2D, dash-dotted curve) due to leakage of the encapsulated dye into the external solution and consequently reduced self-quenching.[16]

Figure 3 shows a schematic model of an amphiphilic GQD unilamellar vesicle, based on the microscopy and spectroscopy experiments outlined in Figure 2. In the model, the amphiphilic GQDs adopt a bilayer arrangement in which the extended hydrocarbon chains constitute the hydrophobic layer, while the graphene cores, the surfaces of which are partially derivatized with carboxyl and hydroxyl residues, form the hydrophilic domains exposed to the aqueous solution. Analogous to conventional lipid vesicles, the unilamellar amphiphilic GQD bilayer separates the enclosed aqueous volume from the external solution (Figure 3).

The photoluminescence properties of the amphiphilic GQDs can be exploited for microscopic imaging and spectroscopic applications (Figure 4). Figure 4A shows multicolor fluorescence confocal microscopy images of the unilamellar GQD vesicles, obtained by employing four different excitation/emission wavelengths. The broad GQD excitation/emission range that is apparent in the confocal micrographs in Figure 4A suggests possible use of the vesicles in imaging experiments by selection of suitable excitation wavelengths and emission filters.

Figure 4B illustrates the use of giant amphiphilic GQD vesicles for investigating the temporal evolution of membrane events in situ. Figure 4B shows micrographs of a single GQD

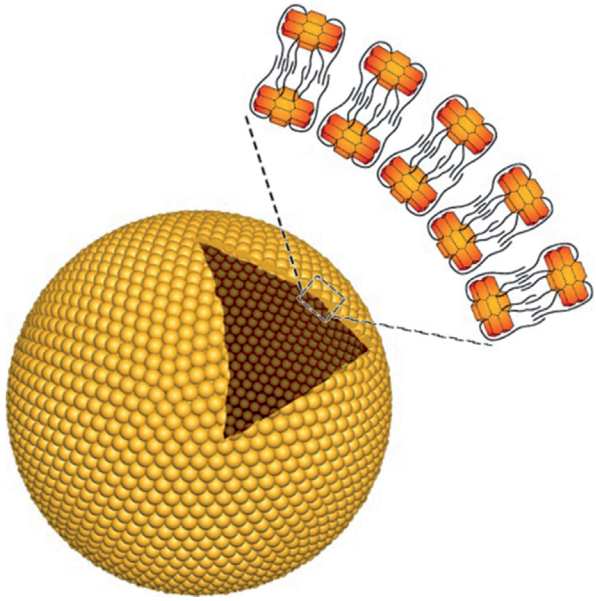

Figure 3. Schematic model of the unilamellar amphiphilic GQD vesicles. The model is based upon the experimental data in Figures 1 and 2 and shows the bilayer unilamellar lamellar organization of the amphiphilic GQDs making up the vesicle wall. The graphene cores of the individual GQDs (orange) form the external bilayer surface, while the hydrophobic acyl chains, shown in black, form the hydrophobic internal layer.

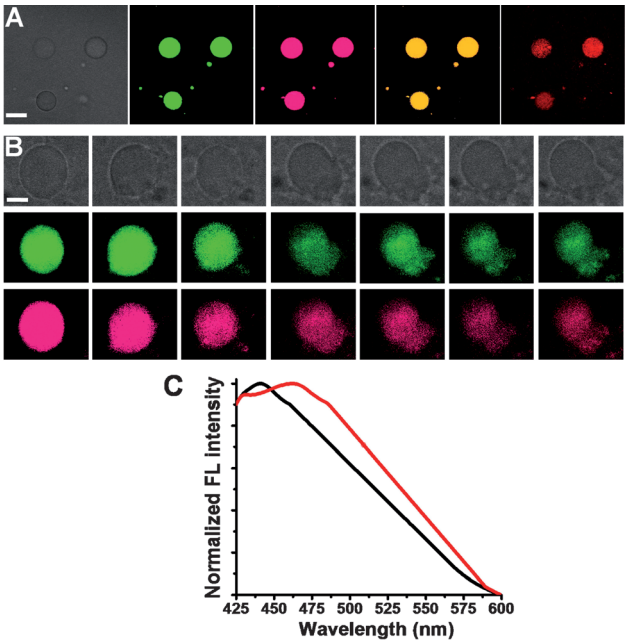

Figure 4. Fluorescence microscopy and spectroscopy of the amphiphilic GQD vesicles. A) Confocal micrographs of amphiphilic GQD vesicles. Bright-field image (top left) and fluorescence images recorded on excitation at 440 nm with emission filter EM 477/45 (green); excitation at 488 nm, emission filter EM 525/50 (magenta); excitation at 514 nm, emission filter EM 525/50 (orange); and excitation at 568 nm, emission filter EM 640/120H (red). Scale bar: 10 μm. B) Bright field (top) and fluorescence images of a single amphiphilic GQD vesicle on excitation at 440 nm (emission filter EM 477/45; green) and 488 nm (emission filter EM 525/50; magenta) before and after addition of Aβ40. Images from left to right: the GQD vesicle before peptide addition (control) and 1, 5, 10, 15, 20, and 30 min after addition of the peptide to the vesicle solution, respectively. Scale bar: 5 μm. C) Fluorescence emission spectra (excitation at 375 nm) of amphiphilic GQD vesicles before (black) and after (red) addition of Aβ40.

vesicle recorded at different times after addition of the peptide beta-amyloid (1–40) (Aβ40), in the monomeric form, to a solution of unilamellar amphiphilic GQD vesicles. Micrographs were recorded in bright-field mode and at two excitation/emission wavelengths. Aβ40 is believed to be a prominent toxic factor in Alzheimer's disease, and interactions of the peptide with membrane bilayers have been recorded. Indeed, the micrographs in Figure 4B provide a real-time visual demonstration of gradual Aβ40-induced distortion of the spherical membrane surface, which results in significantly deformed vesicle morphology.

Membrane interactions of the peptide can be also elucidated by fluorescence spectroscopy. Figure 4C depicts the fluorescence emission peak (375 nm excitation) of a solution of amphiphilic GQD vesicles recorded before and after incubation of the vesicles with Aβ40. Notably, a clear shift to a higher emission wavelength was induced by Aβ40, reflecting vesicle binding and the significant bilayer distortion induced by the peptide.

Conclusion

We have demonstrated formation of unilamellar vesicles through spontaneous self-assembly of amphiphilic graphene quantum dots as the sole building blocks. The vesicles, which span sizes of hundreds of nanometers (large unilamellar vesicles) to micrometers (giant unilamellar vesicles) closely resemble conventional lipid vesicles in their size and morphology. Indeed, the GQDs adopt a bilayer organization, that is, the amphiphilic nature of these carbonaceous nanoparticles dictates formation of microscale self-assembled structures. Notably, the photoluminescence properties of the GQD building blocks provide a powerful analytical platform for investigating membranes and membrane interactions. The new amphiphilic GQD vesicle system could be exploited in microscopic and spectroscopic studies on membrane properties and membrane-associated processes.

Experimental Section

Materials and methods

All chemicals were purchased from Sigma-Aldrich and used without further purification. All solvents were of HPLC grade. Beta-amyloid (1–40) (Aβ40) with the amino acid sequence DAEFRHDSGYEVHHQKLVFFAEDVGSNKGAIIGLMVGGVVIATVIVI was purchased from Peptron (South Korea) in lyophilized form at >90% purity (HPLC). 1,1,1,3,3,3-Hexafluoro-2-propanol and sodium phosphate monobasic were purchased from Sigma-Aldrich (Rehovot, Israel). Fluorescein 5-isothiocyanate (FITC) was purchased from Invitrogen (Eugene, Oregon, USA). Confocal micrographs were acquired with a PerkinElmer Ultra VIEW system (PerkinElmer Life Sciences Inc., MA, USA) equipped with Axiovert 200M (Zeiss, Germany) microscope and a Plan-Neofluar 63×/1.4 NA oil objective.

Synthesis of GQDs: A mixture of concentrated sulfuric acid (20 mL) and concentrated nitric acid (6.3 mL) was placed with 100 mg of carbon fibers in a 100 mL round-bottom flask fitted with a reflux condenser. The mixture was sonicated for about 4 h and then stirred at 95 °C for 24 h. After completion of the reaction, the mixture was cooled to room temperature, diluted with double-distilled water (400 mL), and the pH of the solution was adjusted to 7 by adding Na_2CO_3. The solution was then kept at 4 °C for 12 h, followed by centrifugation at 4 °C for 30 min (4000 rpm). The supernatant was decanted to get rid of byproducts. The product was then purified by dialysis for 3 d by using a dialysis bag with a molecular weight cutoff of 12000 Dalton. The purified product was then freeze-dried to give pure graphene quantum dots (compound **1** in Figure 1 of the Supporting Information).

Synthesis of amphiphilic GQDs: GQDs were dissolved in DMF (250 mL) in a round-bottomed flask and 1-octadecanol (10 g) was added. The mixture was heated to 95 °C with stirring and kept at 95 °C for 3 d. The mixture was then ice-cooled and filtered to remove the unconsumed 1-octadecanol. The filtrate was then collected. The product was extracted with ethyl acetate, washed four times with brine (each time 200 mL), dried over sodium sulfate, and the organic solvent was removed under reduced pressure to obtain pure amphiphilic GQDs.

Assembly of amphiphilic GQD vesicles: An amount of amphiphilic GQDs (5 mg) was dissolved in clean chloroform (500 μL) by vortexing (for about 15 min) and sonication (for about 30 min). The solution was then transferred to a 250 mL round-bottom flask and the aqueous phase (1.5 mL of 0.1 M sucrose, 0.1 mM KCl, 50 mM Tris solution, pH 7.4) was then carefully added along the flask wall while stirring gently with a plastic pipette for about 6 min. The organic solvent was then removed on a rotary evaporator under reduced pressure (final pressure 20 mbar) at room temperature. After evaporation for 4–5 min, an opalescent fluid was obtained with a volume of approximately 1.5 mL.

Aβ40 peptide: Aβ40 was dissolved in 1,1,1,3,3,3-hexafluoropropan-2-ol at a concentration of 1 mg mL^{-1} and the solution stored at −20 °C until use to prevent fibril formation. For experiments the solution was thawed, and the required amount was dried by evaporation for 6–7 h to remove the HFIP. The dried peptide monomer samples were dissolved in NaH_2PO_4 buffer (10 mM), pH 7.4, at room temperature. For confocal fluorescent microscopy, Aβ40 monomer (0.3 mM) was dissolved in NaH_2PO_4 buffer, and 10 μL of the monomer solution was then immediately added to the amphiphilic GQDs vesicles. In the fluorescence spectroscopy experiment, Aβ40 was dissolved in NaH_2PO_4 buffer (20 μL) and the solution was added to a quartz cuvette containing vesicle solution (1 mL).

Characterization

Size distribution and HRTEM study on the as-synthesized amphiphilic GQDs: Size distributions and HRTEM images were obtained by using a 200 kV JEOL JEM-2100F microscope. For HRTEM studies, 0.5 mg of the as-synthesized amphiphilic GQDs was dissolved in 500 μL of chloroform, the solution centrifuged at 14000 rpm for 10 min, and the centrifugate collected. 10 μL of freshly prepared centrifugate was placed on an ultrathin carbon-film-coated copper grid, dried at room temperature for 2 h, and analyzed by HRTEM. The size distribution of the particles was calculated from 50 randomly chosen particles in the HRTEM image (Figure 1 A) by using Image J software. Particle distribution was plotted on the basis of these statistics by using OriginPro software (Version 8.5).

AFM: AFM analysis was carried out with a Dimension 3100 SPM Digital Instruments (Veeco, NY, USA). The surface morphology of the GQDs was investigated by analyzing a sample prepared by transferring a monolayer of amphiphilic GQDs from the air/water interface at a surface pressure of 8 mN m^{-1} onto a mica substrate by the Langmuir–Blodgett technique. The thickness distribution of the nanoparticles was calculated by using NanoScope Analysis v1.40 software, and the statistical distribution was plotted with OriginPro software (Version 8.5).

Fluorescence spectroscopy: Steady-state fluorescence spectra were recorded with a JASCO FP-8300 spectrofluorometer.

Cryo-TEM: Cryo-TEM imaging of the amphiphilic GQD vesicles was carried out according to the following procedure: In the controlled-environment box of a vitrification robot (Vitrobot), a drop of the vesicle solution was deposited on a glow-discharged TEM grid (300 mesh Cu Lacey substrate; Ted Pella, Ltd.). The excess liquid was automatically blotted with a filter paper, and the specimen was rapidly plunged into liquid ethane and transferred to liquid nitrogen, where it was kept until used. The samples were examined below −175 °C by using an FEI Tecnai 12 G2 TWIN TEM operated at 120 kV in low-dose mode and at a few micrometers under focus to increase phase contrast. The images were recorded with a Gatan charge-coupled device camera (model 794) and analyzed by Digital Micrograph software, Version 3.1.

Cryo-SEM: A sample of GQD vesicle solution (1.5 μL) was sandwiched between two flat aluminum platelets with a 200 mesh TEM grid used as a spacer. The sample was then frozen at high pressure in an HPM010 high-pressure freezing machine (Bal-Tec, Liechtenstein). The frozen samples were mounted on a holder and transferred to a BAF 60 freeze-fracture device (Leica Microsystems, Austria) using a VCT 100 (Vacuum Cryo Transfer device, Leica Microsystems, Austria). After fracturing at a temperature of −120 °C, samples were transferred to an Ultra 55 SEM (Zeiss, Germany) by using a VCT 100 and observed with a secondary-electrons in-lens detector at an acceleration voltage of 1 kV. Water was sublimed during observation at a temperature of −105 °C.

Fluorescent leakage experiment: FITC stock solution (1.52 mM) was prepared in chloroform/ethanol (1/1, v/v). A sample of amphiphilic GQDs (5 mg) was dissolved in chloroform (1000 μL) in a 4 mL glass vial by vortexing (for about 15 min) and sonication (for about 30 min), FITC stock solution (4.93 μL) was subsequently added, and the mixture was mixed by vortexing and sonication. The monodisperse solution was then transferred to a 250 mL round-bottom flask and the aqueous phase (1.5 mL of 0.1 M sucrose, 0.1 mM KCl, 50 mM Tris solution, pH 7.4) was then slowly and carefully added along the flask walls and the mixture stirred gently with a plastic pipette for about 6 min. The organic solvent was removed on a rotary evaporator under reduced pressure (final pressure 20 mbar) at room temperature. After evaporation for 4–5 min, an opalescent fluid was obtained with a volume of approximately 1.5 mL. The vesicle solution was then filtered through a 200 nm PVDF Millipore membrane filter unit and the residue was washed with aqueous phase (1.5 mL of 0.1 M sucrose, 0.1 mM KCl, 50 mM Tris solution, pH 7.4) and redispersed in aqueous phase (1.5 mL of 0.1 M sucrose, 0.1 mM KCl, 50 mM Tris solution, pH 7.4). A sample (1 mL) of the GVs solution was taken in a quartz cuvette and sub-

jected to fluorescent leakage studies before and after the addition of Triton X-100 (10 μL of 10% (w/v)).

SAXS: A sample of amphiphilic GQDs (10 mg) was dissolved in chloroform (250 μL) and the solution dried overnight in a test tube. The dry film of amphiphilic GQDs was then hydrated in water to get multilamellar vesicles, which were then subjected to SAXS study. Samples for SAXS study were prepared by filling thin glass capillaries (1.5 mm in diameter) and sealing them with epoxy glue. A SAXSLAB GANESHA 300-XL was used for SAXS measurements. $Cu_{K\alpha}$ radiation was generated by a Genix 3D Cu source (operated at 47 kV and 5.7 mA) with an integrated monochromator, three-pinhole collimator, and a Pilatus 300K two-dimensional detector. The distance between the sample and detector was 350 mm.

Confocal fluorescence microscopy: Confocal micrographs of amphiphilic GQD vesicles were acquired on a PerkinElmer UltraVIEW system (PerkinElmer Life Sciences Inc., MA, USA) equipped with Axiovert 200M microscope (Zeiss, Germany) and a 63×/1.4 NA Zeiss Plan-Apochromat oil-immersion objective. The excitation wavelengths of 440, 488, 514, and 568 nm were produced by an argon/krypton laser.

Acknowledgements

The Kreitman School of Advanced Graduate Studies at Ben Gurion University is acknowledged for financial support (S.N.).

Keywords: amphiphiles · graphene · membranes · quantum dots · vesicles

[1] a) J. Peng, W. Gao, B. K. Gupta, Z. Liu, R. Romero-Aburto, L. Ge, L. Song, L. B. Alemany, X. Zhan, G. Gao, S. A. Vithayathil, B. A. Kaipparettu, A. A. Marti, T. Hayashi, J.-J. Zhu, P. M. Ajayan, *Nano Lett.* **2012**, *12*, 844 – 849; b) G. E. LeCroy, S. K. Sonkar, F. Yang, L. M. Veca, P. Wang, K. N. Tackett, J.-J. Yu, E. Vasile, H. Qian, Y. Liu, P. Luo, Y.-P. Sun, *ACS Nano* **2014**, *8*, 4522 – 4529; c) L. M. Veca, A. Diac, I. Mihalache, P. Wang, G. E. LeCroy, E. M. Pavelescu, R. Gavrila, E. Vasile, A. Terec, Y.-P. Sun, *Chem. Phys. Lett.* **2014**, *613*, 40 – 44; d) E. Muro, T. Pons, N. Lequeux, A. Fragola, N. Sanson, Z. Lenkei, B. Dubertret, *J. Am. Chem. Soc.* **2010**, *132*, 4556 – 4557.

[2] M. Chen, W. Wang, X. Wu, *J. Mater. Chem. B* **2014**, *2*, 3937 – 3945.

[3] A. Salinas-Castillo, M. Ariza-Avidad, C. Pritz, M. Camprubi-Robles, B. Fernandez, M. J. Ruedas-Rama, A. Megia-Fernandez, A. Lapresta-Fernandez, F. Santoyo-Gonzalez, A. Schrott-Fischer, L. F. Capitan-Vallvey, *Chem. Commun.* **2013**, *49*, 1103 – 1105.

[4] L. Feng, X.-Y. Tang, Y.-X. Zhong, Y.-W. Liu, X.-H. Song, S.-L. Deng, S.-Y. Xie, J.-W. Yan, L. Zheng, *Nanoscale* **2014**, *6*, 12635 – 12643.

[5] a) M. Nurunnabi, Z. Khatun, G. R. Reeck, D. Y. Lee, Y.-k. Lee, *Chem. Commun.* **2013**, *49*, 5079 – 5081; b) D. B. Shinde, V. K. Pillai, *Angew. Chem. Int. Ed.* **2013**, *52*, 2482 – 2485; *Angew. Chem.* **2013**, *125*, 2542 – 2545; c) A. B. Bourlinos, A. Stassinopoulos, D. Anglos, R. Zboril, M. Karakassides, E. P. Giannelis, *Small* **2008**, *4*, 455 – 458; d) K. K. R. Datta, O. Kozak, V. Ranc, M. Havrdova, A. B. Bourlinos, K. Safarova, K. Hola, K. Tomankova, G. Zoppellaro, M. Otyepka, R. Zboril, *Chem. Commun.* **2014**, *50*, 10782 – 10785.

[6] S. Zhu, J. Zhang, C. Qiao, S. Tang, Y. Li, W. Yuan, B. Li, L. Tian, F. Liu, R. Hu, H. Gao, H. Wei, H. Zhang, H. Sun, B. Yang, *Chem. Commun.* **2011**, *47*, 6858 – 6860.

[7] S. Nandi, R. Malishev, K. Parambath Kootery, Y. Mirsky, S. Kolusheva, R. Jelinek, *Chem. Commun.* **2014**, *50*, 10299 – 10302.

[8] J. Wang, C.-F. Wang, S. Chen, *Angew. Chem. Int. Ed.* **2012**, *51*, 9297 – 9301; *Angew. Chem.* **2012**, *124*, 9431 – 9435.

[9] a) S. A. Kotler, P. Walsh, J. R. Brender, A. Ramamoorthy, *Chem. Soc. Rev.* **2014**, *43*, 6692 – 6700; b) T. Ikenoue, Y.-H. Lee, J. Kardos, H. Yagi, T. Ikegami, H. Naiki, Y. Goto, *Proc. Natl. Acad. Sci. USA* **2014**, *111*, 6654 – 6659; c) U. H. N. Dürr, M. Gildenberg, A. Ramamoorthy, *Chem. Rev.* **2012**, *112*, 6054 – 6074; d) M. F. M. Sciacca, Samuel A. Kotler, J. R. Brender, J. Chen, D.-k. Lee, A. Ramamoorthy, *Biophys. J.* **2012**, *103*, 702 – 710.

[10] J. Shen, Y. Zhu, X. Yang, C. Li, *Chem. Commun.* **2012**, *48*, 3686 – 3699.

[11] T. Takahiro, O. Toshio, *Appl. Phys. Express* **2009**, *2*, 075502.

[12] A. Moscho, O. Orwar, D. T. Chiu, B. P. Modi, R. N. Zare, *Proc. Natl. Acad. Sci. USA* **1996**, *93*, 11443 – 11447.

[13] M. Fidorra, A. Garcia, J. H. Ipsen, S. Härtel, L. A. Bagatolli, *Biochim. Biophys. Acta, Biomembr.* **2009**, *1788*, 2142 – 2149.

[14] a) Z. Nie, A. Petukhova, E. Kumacheva, *Nat. Nanotechnol.* **2010**, *5*, 15 – 25; b) M. S. Nikolic, C. Olsson, A. Salcher, A. Kornowski, A. Rank, R. Schubert, A. Frömsdorf, H. Weller, S. Förster, *Angew. Chem. Int. Ed.* **2009**, *48*, 2752 – 2754; *Angew. Chem.* **2009**, *121*, 2790 – 2792; c) S. Park, J.-H. Lim, S.-W. Chung, C. A. Mirkin, *Science* **2004**, *303*, 348 – 351; d) A. D. Duong, G. Ruan, K. Mahajan, J. O. Winter, B. E. Wyslouzil, *Langmuir* **2014**, *30*, 3939 – 3948; e) P. Huang, J. Lin, W. Li, P. Rong, Z. Wang, S. Wang, X. Wang, X. Sun, M. Aronova, G. Niu, R. D. Leapman, Z. Nie, X. Chen, *Angew. Chem. Int. Ed.* **2013**, *52*, 13958 – 13964; *Angew. Chem.* **2013**, *125*, 14208 – 14214.

[15] J. Lee, K. Kim, W. I. Park, B.-H. Kim, J. H. Park, T.-H. Kim, S. Bong, C.-H. Kim, G. Chae, M. Jun, Y. Hwang, Y. S. Jung, S. Jeon, *Nano Lett.* **2012**, *12*, 6078 – 6083.

[16] E. E. Ambroggio, F. Separovic, J. H. Bowie, G. D. Fidelio, L. A. Bagatolli, *Biophys. J.* **2005**, *89*, 1874 – 1881.

Received: November 21, 2014
Published online on March 20, 2015